Characterization of Lesions and Regional Brain Tissue of ArcAbeta Mice Based on Magnetic Susceptibility

A. Deistung[1], J. Klohs[2], F. Schweser[1], J. Grandjean[2], M. Dominietto[2], C. Waschkies[2], R. M. Nitsch[3], M. Rudin[2,4], and J. R. Reichenbach[1]
[1]Medical Physics Group, Department of Diagnostic and Interventional Radiology I, Jena University Hospital, Jena, Germany, [2]Institute for Biomedical Engineering, ETH & University of Zürich, Switzerland, [3]Division of Psychiatry Research, University of Zürich, Switzerland, [4]Institute of Pharmacology and Toxicology, University of Zürich, Switzerland

Introduction

Alzheimer's disease (AD) is a slowly progressing neurodegenerative disorder and is characterized by the formation of amyloid-β plaques in brain tissue. Recently, Wengenack et al. [1] investigated the iron load of amyloid plaques in AD transgenic mice brains (APP/PS1). The authors found regional iron-load differences with decreased levels in cortical and hippocampal plaques compared to thalamic plaques. Since magnetic voxel susceptibility is supposed to be proportional to the iron load, quantitative magnetic susceptibility mapping (QSM), a novel technique based on gradient echo (GRE) phase data, may potentially be applied to non-invasively assess this lesion iron distribution. Therefore, the current study aims at optimizing QSM for high resolution MR imaging of mice brains and evaluating its potential to characterize the punctuate lesions in the brain of arcAβ mice. Furthermore, the regional differences of the brain tissue iron load are investigated in both living transgenic arcAβ mice and wild type (wt) controls.

Material and Methods

Data Acquisition and Processing: High-resolution brain data of transgenic arcAβ mice ($n_{arcA\beta} = 3$) and wt controls ($n_{wt} = 6$) at 16 months of age were acquired in horizontal orientation with a 3D fully flow compensated GRE sequence (TE/TR/FA=12ms/250ms/15°, voxel size 60×60×60 µm³) on a 9.4T small animal MRI system (BioSpec, Bruker Biospin MRI, Ettlingen, Germany) using a cryogenic quadrature surface RF probe [2]. Phase aliasing was resolved by 3D phase unwrapping [3]. Background phase contributions were eliminated by the projection onto dipole field technique [4,5], and the relative difference field (RDF) was computed by dividing the background-corrected phase with the echo time, gyromagnetic ratio for protons, and the magnetic field strength of the MRI system. The following optimization problem was solved to obtain the susceptibility maps: $\min_{\chi,\sigma} = \|A\chi + \alpha\sigma - RDF\|_2^2 + \beta\|WG\chi\|_2^2$. The first term is the squared distance between the RDF and the fitted field $A\chi + \alpha\sigma$, where $A\chi$ replicates the RDF due to the susceptibility distribution χ, and σ denotes a local offset [6]. The second term is the weighted gradient of the magnetic susceptibility distribution χ as proposed by de Rochefort et al. [5]. The scalar coefficients $\alpha = 1$ and β are regularization parameters.

Data Analysis: Volumes of interest (VOIs) were identified on magnitude images in regions of cortex, hippocampus, thalamus, and cerebrospinal fluid (CSF) taking care that lesions were excluded. VOIs were identified for lesions located in the cortex, hippocampus, thalamus, and olfactory bulb in arcAβ mice. Finally, a statistical analysis was performed on the voxel values of the VOIs with respect to differences of brain tissue susceptibility between arcAβ and wt mice as well as lesion location. This analysis included calculation of mean values of the susceptibility difference with respect to CSF, box plots, and two-sampled *t*-tests.

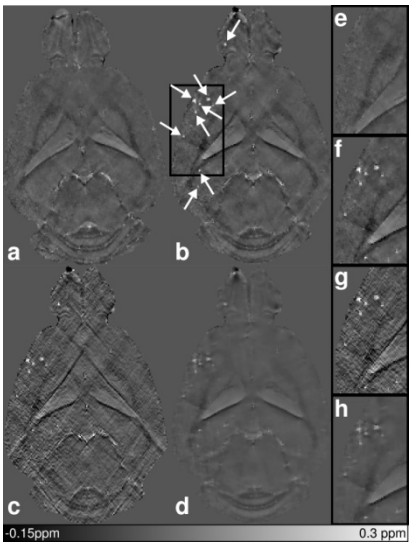

Figure 1: *The upper row (a,b,e,f) presents similar regions of susceptibility maps of a wild type (a,e) and an arcAβ (b,f) mouse computed with β=0.5. The influence of β on the resulting susceptibility map is demonstrated for the same arcAβ data set in the lower row (c,d,g,h), where susceptibility maps computed with β=0.05 and β=2.3 are shown in (c,g) and (d,h), respectively. The right column (e-h) illustrates enlarged sections of the susceptibility maps, highlighted by the black box in (b).*

Results

Susceptibility maps of an arcAβ mouse and wt control calculated with different regularization parameters β are displayed in Fig. 1(b-d, f-h), indicating the need for proper adjustment of β. Small β resulted in sharp images with streaking artifacts (Fig. 1c,g), whereas large β resulted in smoothing of susceptibility maps accompanied by loss of contrast between adjacent tissue structures (Fig. 1d,h), demonstrating the trade-off between artifact level and contrast. In a systematic VOI-based analysis (not shown) $\beta = 0.5$ was found to yield the best trade-off. Comparison of the susceptibility maps of a wild type (Fig. 1a,e) and an arcAβ mouse (Fig. 1b,f) reveals the occurrence of paramagnetic (hyperintense) punctuate lesions in the arcAβ mouse model (see arrows in Fig 1b). The mean susceptibilities of 53 cortical, 6 hippocampal, 31 thalamic, and 6 olfactory bulb lesions that were identified in arcAβ mice were (101.2 ± 47.5) ppb, (76.7 ± 52.8) ppb, (80.4 ± 53.3) ppb, and (140.2 ± 36.2) ppb, respectively. The boxplot in Figure 2 emphasizes increasing lesion susceptibilities from hippocampus over thalamus and cortex to the olfactory bulb. Only the lesions in the olfactory bulb had a susceptibility significantly different from the hippocampal ($p = 0.035$) and thalamic ($p = 0.012$) lesions. VOI-based analysis of cortical, hippocampal, thalamic and white matter tissue revealed no significant differences in susceptibilities between brain regions in arcAβ compared to wt mice (Tab. 1).

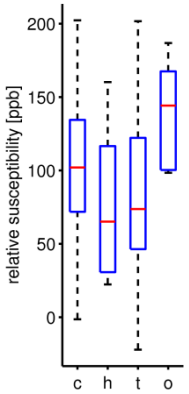

Figure 2: *Box plot of lesion susceptibilities measured in the cortex (c), hippocampus (h), thalamus (t), and olfactory bulb (o).*

Discussion & Conclusion

We have presented preliminary results for application of QSM to wt and arcAβ mice. The small trend of regional variances of magnetic susceptibility in lesions may be attributed to the limited number of investigated arcAβ mice and lesions, as well as the fact that lesion sizes were in the range of the MRI resolution in most cases. The observed deviation of the findings to Wengenack et al. [1] may be attributed to a different mouse model employed. In the arcAβ mice the identified lesions could either be microbleeds or plaques. These two lesion types contain different amounts of iron and, hence, have different susceptibility values. Another reason for susceptibility variations might be attributed to differences in the composition, iron load and microscopic morphology of the lesions in the mouse models. It has been shown with electron microscopy in APP/PS1 transgenic AD mice that thalamic plaques have a globular structure of concentric layers (spherical plaques) [7,8], whereas other plaques (cortical/hippocampal plaques) have radially oriented fibrils (fibrillar plaques) [9], indicating potential differences in the β-sheet structure among the plaques. These differences in tissue microstructures may also affect susceptibility values among plaques, as anisotropic microscopic tissue magnetic architecture [10] and anisotropic magnetic susceptibility [11,12] produce orientation dependent contributions to the phase signal, which are not considered by the applied QSM technique. These aspects will be addressed in future studies with histological analysis of the sections. Furthermore, the direct relationship of measured magnetic susceptibility with iron in tissue and plaques will be quantified by using inductively coupled plasma-mass spectroscopy (ICP-MS) or atomic absorption spectroscopy (AAS). Nevertheless, QSM is a suitable tool to investigate variations of iron load in longitudinal studies in patients with AD or other neurological diseases.

brain region	arcAβ	wild type	p-value
cortex	-31.6 ± 7.8	-33.9 ± 7.3	0.55
hippocampus	-32.4 ± 7.2	-38.6 ± 9.3	0.17
thalamus	-19.5 ± 6.0	-25.2 ± 7.4	0.12
white matter	-55.8 ± 9.9	-59.0 ± 7.3	0.44

Table 1: *VOI-based susceptibilities of brain tissue (in ppb).*

References

[1] Wengenack TM, et al, Neuroimage. 2011;54(1):113-122. [2] Baltes C, et al. NMR Biomed. 2009;22(8):834-842. [3] Abdul-Rahman HS, et al. *Appl Opt*. 2007;46(26):6623-3. [4] Liu T, et al. Proc. of ISMRM. 2010:141. [5] de Rochefort L, et al. Magn Reson Med. 2010;63(1):194-206. [6] Schweser F, et al. Med Phys. 2010;37(9):5165-5178. [7] Dhenain M, et al. NMR Biomed. 2002;15(3):197-203. [8] Dhenain M, et al. Neurobiol Aging. 2009;30(1):41-53. [9] Sasaki A, et al. Virchows Arch. 2002;441(4):358-367. [10] He X and Yablonksiy DA. Proc Natl Acad Sci USA. 2009;106(32):13558-13563. [11] Liu C. Magn Reson Med. 2010;63(6):1471-7. [12] Lee J, et al. Proc Natl Acad Sci USA. 2010;107(11):5130-5.